J|A|C|S ARTICLES

Published on Web 10/22/2010

Hierarchical Self-Assembly of a Biomimetic Diblock Copolypeptoid into Homochiral Superhelices

Hannah K. Murnen,[†] Adrianne M. Rosales,[†] Jonathan N. Jaworski,[§] Rachel A. Segalman,*[,†,‡] and Ronald N. Zuckermann*[,‡,§]

Department of Chemical and Biomolecular Engineering, University of California, Berkeley, California 94720, and Molecular Foundry, Materials Science Division, Lawrence Berkeley National Laboratory, 1 Cyclotron Road, Berkeley, California 94720

Received July 16, 2010; E-mail: rnzuckermann@lbl.gov; segalman@berkeley.edu

Abstract: The aqueous self-assembly of a sequence-specific bioinspired peptoid diblock copolymer into monodisperse superhelices is demonstrated to be the result of a hierarchical process, strongly dependent on the charging level of the molecule. The partially charged amphiphilic diblock copolypeptoid 30-mer, [*N*-(2-phenethyl)glycine]$_{15}$-[*N*-(2-carboxyethyl)glycine]$_{15}$, forms superhelices in high yields, with diameters of 624 $\pm$ 69 nm and lengths ranging from 2 to 20 μm. Chemical analogs coupled with X-ray scattering and crystallography of a model compound have been used to develop a hierarchical model of self-assembly. Lamellar stacks roll up to form a supramolecular double helical structure with the internal ordering of the stacks being mediated by crystalline aromatic side chain−side chain interactions within the hydrophobic block. The role of electrostatic and hydrogen bonding interactions in the hydrophilic block is also investigated and found to be important in the self-assembly process.

Introduction

Hierarchical self-assembly is a hallmark of biological materials. Systems ranging from nacre[1] to collagen fibrils[2] have been heralded for their mechanical strength stemming from their unique layered structures. The precise order of these biomaterials on the micrometer and millimeter scales arises from atomically defined interactions at the nanometer and even subnanometer level. Understanding the relationship between these interactions has great implications for the design of new materials with controllable order across many length scales.[3]

Although examples of hierarchical polypeptide structures abound in nature,[4−6] the *de novo* design of such systems is still a major challenge.[7] While progress has been made in the design of simple polypeptide motifs, the molecular complexity of polypeptide interactions makes it difficult to engineer their self-assembly into complex or hierarchical structures. Hydrophobic and ionic forces are joined by backbone chirality and hydrogen bonding, making it challenging to isolate or understand the effect of any parameter in particular. Thus, most efforts in the *de novo* design of folded and self-assembling peptides have focused on relatively short chain lengths.[8−14] The utility of engineered peptide structures in the design of structured biomaterials has been proven by the diversity of achievable structures including flat or twisted tapes, tubes, and spheres,[13,15] as well as by the insights gained into the mechanisms of amyloid[16,17] and collagen[11,12,18] fibril formation. *De novo* peptide systems are thus attractive for specific biotechnological applications,[3] but simpler biomimetic polymer systems may allow the development of straightforward design rules for the engineering of self-assembled materials. Therefore, a tunable and synthetically robust system that can mimic the atomic level ordering in biological systems while allowing system engineering is desired for both materials applications and fundamental investigations of biomacromolecular self-assembly.

[†] University of California.
[‡] Materials Science Division, Lawrence Berkeley National Laboratory.
[§] Molecular Foundry, Lawrence Berkeley National Laboratory.

(1) Fritz, M.; Morse, D. E. *Curr. Opin. Colloid Interface Sci.* **1998**, *3*, 55–62.
(2) Ottani, V.; Martini, D.; Franchi, M.; Ruggeri, A.; Raspanti, M. *Micron* **2002**, *33*, 587–596.
(3) Rajagopal, K.; Schneider, J. P. *Curr. Opin. Struct. Biol.* **2004**, *14*, 480–486.
(4) Wong, G. C. L.; Tang, J. X.; Lin, A.; Li, Y. L.; Janmey, P. A.; Safinya, C. R. *Science* **2000**, *288*, 2035–2039.
(5) Raviv, U.; Needleman, D. J.; Li, Y. L.; Miller, H. P.; Wilson, L.; Safinya, C. R. *Proc. Natl. Acad. Sci. U.S.A.* **2005**, *102*, 11167–11172.
(6) Audette, G. F.; van Schalk, E. J.; Hazes, B.; Irvin, R. T. *Nano Lett.* **2004**, *4*, 1897–1902.
(7) Schueler-Furman, O.; Wang, C.; Bradley, P.; Misura, K.; Baker, D. *Science* **2005**, *310*, 638–642.
(8) Lamm, M. S.; Rajagopal, K.; Schneider, J. P.; Pochan, D. J. *J. Am. Chem. Soc.* **2005**, *127*, 16692–16700.
(9) Venkatraman, J.; Shankaramma, S. C.; Balaram, P. *Chem. Rev.* **2001**, *101*, 3131–3152.
(10) Saiani, A.; Mohammed, A.; Frielinghaus, H.; Collins, R.; Hodson, N.; Kielty, C. M.; Sherratt, M. J.; Miller, A. F. *Soft Matter* **2009**, *5*, 193–202.
(11) Fallas, J. A.; O'Leary, L. E. R.; Hartgerink, J. D. *Chem. Soc. Rev.* **2010**, *39*, 3510–3527.
(12) Khew, S. T.; Tong, Y. W. *Biochemistry* **2008**, *47*, 585–596.
(13) Adams, D. J.; Holtzmann, K.; Schneider, C.; Butler, M. F. *Langmuir* **2007**, *23*, 12729–12736.
(14) Nagarkar, R. P.; Hule, R. A.; Pochan, D. J.; Schneider, J. P. *J. Am. Chem. Soc.* **2008**, *130*, 4466–4474.
(15) Gazit, E. *Chem. Soc. Rev.* **2007**, *36*, 1263–1269.
(16) Marini, D. M.; Hwang, W.; Lauffenburger, D. A.; Zhang, S. G.; Kamm, R. D. *Nano Lett.* **2002**, *2*, 295–299.
(17) de la Paz, M. L.; Goldie, K.; Zurdo, J.; Lacroix, E.; Dobson, C. M.; Hoenger, A.; Serrano, L. *Proc. Natl. Acad. Sci. U.S.A.* **2002**, *99*, 16052–16057.
(18) Woolfson, D. N. *Biopolymers* **2010**, *94*, 118–127.

 10.1021/ja106340f

Polymer scientists have developed comparatively simpler model systems that allow controlled engineering of self-assembled structures in aqueous solution. Charged amphiphilic block copolymers have emerged as a particularly interesting class of nanoscale building blocks due to their ability to build hierarchical levels of structure by drawing upon the interplay between the ionic and hydrophobic interactions.[19,20] For example, the most well studied system in this category, poly(styrene)-*b*-poly(acrylic acid), has been shown to self-assemble into a variety of structures in solution including hierarchical compound micelles, spheres, rods, and vesicles. The identity of the self-assembled structure depends on the solvent and the relative mole fractions of the chargeable block.[21] Additionally, the charges on many ionizable polymers, including poly(acrylic acid), are amphoteric leading to pH dependent supramolecular structures.[22−24] However, while these structures can have internal ordering qualitatively similar to that for biological structures such as amyloid[25] or collagen fibers,[26] the inherent polydispersity in main chain length and lack of sequence specificity pose a fundamental limit for the achievable order on the atomic level.[3] The lack of precise sequence control or the ability to introduce functional monomers (chiral, charged, hydrophobic, etc.) at specific locations means that only changes to entire block chemistries are possible.

Here we use peptoid polymers to explore the aqueous self-assembly of a family of amphiphilic diblock copolymers. Polypeptoid chemistry is attractive as it combines the sequence specificity of biological systems with the simpler intra-/intermolecular interactions, robustness, and synthetic flexibility of traditional polymers. Polypeptoids, or N-substituted glycines, are a class of biomimetic sequence specific polymers synthesized via a solid-supported submonomer method.[27] The backbone is identical to that of a polypeptide, but the side chain is attached to the nitrogen rather than the α carbon. This difference eliminates hydrogen bonding in the backbone and also eliminates the main chain chirality, allowing the control of desired interactions through the introduction of specific side chains. Additionally, the use of a primary amine as the submonomer opens up a wealth of chemical functionalities for the side chains, making it possible to control and fine-tune the intra- and intermolecular forces simply by changing individual side chains.[28] We recently demonstrated, for example, that certain repeating polypeptoid sequence patterns form highly ordered nanosheet bilayers.[29] Polypeptoids are emerging as an ideal system for understanding macromolecular self-assembly and constructing robust materials with atomic level ordering.

Incorporation of chiral groups into a polymer has been used in synthetic systems to influence the handedness of the resulting self-assembled super structures, particularly in helices. Nolte et al. were able to derive chirality in a self-assembled superhelix from the handedness of a helical polyisocyanopeptide building block.[30] In addition to supramolecular chirality arising from molecular chirality, there are also cases where supramolecular helical chirality results from achiral molecules such as small molecules,[31−34] dendrons,[34−37] and liquid crystals.[38−40] In these cases, the chiral self-assembled supramolecular structures are a racemic mixture or are influenced via mechanical forces such as stirring.[33,41] The lack of backbone chirality in polypeptoids allows the introduction of chirality through monomer incorporation only when desired. The sequence specificity of the polypeptoids and the inherent lack of backbone chirality provide a framework for investigating the effects of molecular chirality on supramolecular chirality.

We present here a hierarchically self-assembled superhelix structure with a uniform segment height (606 ± 105 nm) and diameter (624 ± 69 nm) arising from a partially charged amphiphilic diblock copolypeptoid. The superhelices are remarkably homochiral despite the achiral nature of all components. The adaptable chemistry of the system has been used to make systematic changes to the polymer sequence, and from those changes an in-depth understanding of the internal structure and the role of charge location and density in the self-assembly has been obtained. The origin of the chirality has also been investigated, and further work will focus on this issue.

Materials and Methods

Synthesis. Polypeptoids were synthesized on a custom robotic synthesizer or a commercial Aapptec Apex 396 robotic synthesizer on 100 mg of Rink amide polystyrene resin (0.6 mmol/g, Novabiochem, San Diego). All primary amine submonomers, solvents, and reagents described here were purchased from commercial sources and used without further purification. Reagent grade amine submonomers were used with purities 99% or greater. *N*-(2-Carboxyethyl)glycine was made from the *β*-alanine O-*t*Bu ester hydrochloride submonomer. The submonomer was freebased by

(19) Hales, K.; Pochan, D. J. *Curr. Opin. Colloid Interface Sci.* **2006**, *11*, 330–336.
(20) Stuart, M. A. C.; Hofs, B.; Voets, I. K.; de Keizer, A. *Curr. Opin. Colloid Interface Sci.* **2005**, *10*, 30–36.
(21) Zhang, L. F.; Eisenberg, A. *Science* **1995**, *268*, 1728–1731.
(22) Li, G. Y.; Song, S.; Guo, L.; Ma, S. M. *J. Polym. Sci., Polym. Chem.* **2008**, *46*, 5028–5035.
(23) Xue, Y. N.; Huang, Z. Z.; Zhang, J. T.; Liu, M.; Zhang, M.; Huang, S. W.; Zhuo, R. X. *Polymer* **2009**, *50*, 3706–3713.
(24) Gil, E. S.; Hudson, S. M. *Prog. Polym. Sci.* **2004**, *29*, 1173–1222.
(25) Tycko, R. *Curr. Opin. Struct. Biol.* **2004**, *14*, 96–103.
(26) Orgel, J.; Irving, T. C.; Miller, A.; Wess, T. J. *Proc. Natl. Acad. Sci. U.S.A.* **2006**, *103*, 9001–9005.
(27) Figliozzi, G. M.; Goldsmith, R.; Ng, S. C.; Banville, S. C.; Zuckermann, R. N. *Methods Enzymol.* **1996**, *267*, 437–447.
(28) Rosales, A. M.; Murnen, H. K.; Zuckermann, R. N.; Segalman, R. A. *Macromolecules* **2010**, *43*, 5627–5636.
(29) Nam, K. T.; Shelby, S. A.; Choi, P. H.; Marciel, A. B.; Chen, R.; Tan, L.; Chu, T. K.; Mesch, R. A.; Lee, B.-C.; Connolly, M. D.; Kisielowski, C.; Zuckermann, R. N. *Nat. Mater.* **2010**, *9*, 454–460.
(30) Cornelissen, J.; Fischer, M.; Sommerdijk, N.; Nolte, R. J. M. *Science* **1998**, *280*, 1427–1430.
(31) Jeong, K. U.; Jin, S.; Ge, J. J.; Knapp, B. S.; Graham, M. J.; Ruan, J. J.; Guo, M. M.; Xiong, H. M.; Harris, F. W.; Cheng, S. Z. D. *Chem. Mater.* **2005**, *17*, 2852–2865.
(32) Yang, W. S.; Chai, X. D.; Chi, L. F.; Liu, X. D.; Cao, Y. W.; Lu, R.; Jiang, Y. S.; Tang, X. Y.; Fuchs, H.; Li, T. J. *Chem.—Eur. J.* **1999**, *5*, 1144–1149.
(33) Ribo, J. M.; Crusats, J.; Sagues, F.; Claret, J.; Rubires, R. *Science* **2001**, *292*, 2063–2066.
(34) Rosen, B. M.; Wilson, C. J.; Wilson, D. A.; Peterca, M.; Imam, M. R.; Percec, V. *Chem. Rev.* **2009**, *109*, 6275–6540.
(35) Percec, V.; Imam, M. R.; Peterca, M.; Wilson, D. A.; Graf, R.; Spiess, H. W.; Balagurusamy, V. S. K.; Heiney, P. A. *J. Am. Chem. Soc.* **2009**, *131*, 7662–7677.
(36) Percec, V.; Imam, M. R.; Peterca, M.; Wilson, D. A.; Heiney, P. A. *J. Am. Chem. Soc.* **2009**, *131*, 1294–1304.
(37) Peterca, M.; Percec, V.; Imam, M. R.; Leowanawat, P.; Morimitsu, K.; Heiney, P. A. *J. Am. Chem. Soc.* **2008**, *130*, 14840–14852.
(38) Hough, L. E.; Jung, H. T.; Kruerke, D.; Heberling, M. S.; Nakata, M.; Jones, C. D.; Chen, D.; Link, D. R.; Zasadzinski, J.; Heppke, G.; Rabe, J. P.; Stocker, W.; Korblova, E.; Walba, D. M.; Glaser, M. A.; Clark, N. A. *Science* **2009**, *325*, 456–460.
(39) Lin, S. C.; Lin, T. F.; Ho, R. M.; Chang, C. Y.; Hsu, C. S. *Adv. Funct. Mater.* **2008**, *18*, 3386–3394.
(40) Jeong, K. U.; Yang, D. K.; Graham, M. J.; Tu, Y. F.; Kuo, S. W.; Knapp, B. S.; Harris, F. W.; Cheng, S. Z. D. *Adv. Mater.* **2006**, *18*, 3229–3232.
(41) Crusats, J.; El-Hachemi, Z.; Ribo, J. M. *Chem. Soc. Rev.* **2010**, *39*, 569–577.

Table 1. Chemical Structure of the Peptoid Monomers Used and Their Abbreviations

Side chain (R=)	Abbreviation
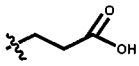	Nce = *N*-(2-carboxyethyl)glycine
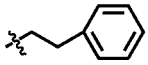	Npe = *N*-(2-phenylethyl)glycine
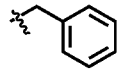	Nbn = *N*-(benzyl)glycine
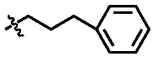	Npp = *N*-(3-phenyl-1-propyl)glycine
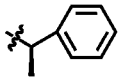	Nrpe = *N*-((R)-(+)-1-phenylethyl)glycine
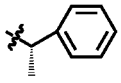	Nspe = *N*-((S)-(-)-1-phenylethyl)glycine
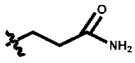	Nbm=*N*-(2-carboxamidoethyl)glycine
	Nme=*N*-(2-methoxyethyl)glycine

extraction from dichloromethane (DCM) and basic water and the resulting compound was confirmed by 1H NMR. A similar procedure was used to freebase the β-alaninamide hydrochloride monomer. In this case the freebase solvent was ethyl acetate/methanol 3:2 (v/v). The polypeptoid synthesis procedure was a modified version of methods previously described[27] using the primary amines shown in Table 1 in a 1.5 M concentration. Displacement times of 60 min were used for the first 15 residues, and 90 min for the remaining residues. All other synthesis conditions were identical to those previously reported.

Peptoid chains were cleaved from the resin by addition of 4.0 mL of trifluoroacetic acid (TFA)/water 95:5 (v/v) for 60 min, which was then evaporated off under a stream of nitrogen gas. This treatment also served to remove the *tert*-butyl protecting groups from the carboxyethyl side chains. Following cleavage, peptoids were dissolved in 4.0 mL of 1:1 (v/v) acetonitrile/water and lyophilized twice to a fluffy white powder.

Each polypeptoid was characterized by analytical reversed-phase HPLC using a C4 column (Vydac 214TP, 5 μm, 4.6 mm $\times$ 150 mm) on a Varian ProStar system (Palo Alto, CA). The column was maintained at 60 °C while a 30 min linear gradient of 5−95% solvent B in solvent A was used (solvent A = 0.1% TFA in water, solvent B = 0.1% TFA in acetonitrile). All peptoids were purified by reversed-phase prep HPLC on a Varian ProStar system equipped with a Varian Model 345 UV−vis Dual Wavelength detector (214 and 260 nm) and a C4 column (Vydac HPLC Protein C4 column, 10−15 μm, 22 mm $\times$ 250 mm) using a linear gradient of 50−100% solvent B in solvent A over 40 min at a flow rate of 10 mL/min (solvent A = 0.1% TFA in water, solvent B = 0.1% TFA in acetonitrile). All of the side chains used are listed in Table 1 along with their abbreviations. Each polymer is named by using the abbreviations of the appropriate side chains along with a subscript indicating the number of repeats of a given monomer in a row. All of the polymers synthesized are shown in Table 2 along with their purities and observed molecular weights. The purity was determined using the analytical reversed-phase HPLC detailed above, and the molecular weight was determined using an Applied Biosystems MALDI TOF/TOF Analyzer 4800 with a 1:1 (v/v) mixture of peptoid (2 mg/mL in 1:1 acetonitrile/water) and 1,8,9-dianthracenetriol (10 mg/ml in tetrahydrofuran).

Table 2. All of the Polymers Synthesized and Used in This Article[a]

Name	Molecular Weight	Observed Molecular Weight	Purity
*p*Npe$_{15}$Nce$_{15}$	4371.5	4372.1	99%
*p*Npe$_{20}$Nce$_{20}$	5823.3	5825.2	99%
*p*Nrpe$_{15}$Nce$_{15}$	4371.5	4365.8	98%
*p*Nspe$_{15}$Nce$_{15}$	4371.5	4377.3	99%
*p*Nce$_{15}$Npe$_{15}$	4371.5	4371.0	98%
*p*Npe$_{14}$Nrpe$_{1}$Nce$_{15}$	4371.5	4371.0	97%
*p*Npe$_{14}$Nspe$_{1}$Nce$_{15}$	4371.5	4372.0	99%
*p*Npp$_{15}$Nce$_{15}$	4582.1	4581.8	96%
*p*Nbn$_{15}$Nce$_{15}$	4161.3	4164.0	ND

[a] The monomers and their abbreviations are shown in Table 1. The subscript in the name indicates the repeat units of that monomer. The observed molecular weights are from MALDI-TOF, and the purity was obtained on an analytical HPLC after prep HPLC purification. ND = not determined.

1,4-Bis-(2-phenethyl)-piperazine-2,5-dione Synthesis and Characterization. The linear dipeptoid was first synthesized on solid phase and then cyclized with heating to form diketopiperazine. 2-Chlorotrityl resin (200 mg; Chem-Impex International, Wood Dale, IL) was swollen for 20 min with DCM and transferred to a manual solid phase reactor. The resin was dried and treated with a solution of bromoacetic acid (1.02 equiv, 45 mg, 0.324 mmol) and diisopropylethylamine (3.34 equiv, 187 μL, 1.07 mmol) in 2 mL of dichloroethane (DCE) and bubbled gently with nitrogen for 1 h. Polypeptoid synthesis was continued with the following modifications. The first displacement was heated at 42 °C overnight, and the second displacement was heated at 37 °C for 6 h. The peptoid was cleaved with 2 mL of 5% (v/v) trifluoroacetic acid in DCM. The crude product was then dissolved in 5 mL of ethanol and heated overnight at 60 °C with stirring to afford cyclization. Solvent was removed *in vacuo* and the product was washed several times with cold ethyl acetate to give 71.3 mg (69% yield based on loading capacity of resin). Mp: 210 °C. ^{1}H NMR (500 MHz, DMSO-d_6, 25 °C): δ = 2.77 (t, $J_{H,H}$ = 7.5 Hz, 4H, CH_2) δ = 3.48 (t, $J_{H,H}$ = 7.5 Hz, 4 H, CH_2), δ = 3.90 (s, 4H, CH_2), δ = 7.18−7.31 (m, 10H, CH) ppm. ^{13}C NMR (500 MHz, DMSO-d_6, 25 °C) δ = 32.36, 46.52, 49.68, 126.30, 128.42, 128.68, 136.75, 163.60.

Self-Assembly Solutions. The amphiphilic molecules were dissolved in water at a concentration between 1 and 10 mg/mL using sodium hydroxide (NaOH) to adjust the pH to the desired value. After pH adjustment, the solutions were allowed to sit at room temperature undisturbed. In order to image the self-assembled structures using AFM or SEM, a drop of solution was placed on an oxygen plasma cleaned silicon wafer. After waiting 10 min, the excess liquid was wicked away and the substrate was washed once with water. To image using TEM, the same technique was used but a carbon-coated copper 200 mesh grid was used instead of the silicon wafer.

X-ray Diffraction. The X-ray diffraction experiments were performed at beamline 8.3.1 and beamline 7.3.3 at the Advanced Light Source at Lawrence Berkeley National Laboratory. Samples were prepared by evaporating the solvent from the solutions using a Genevac. Data presented in the Supporting Information shows that the solid state patterns had identical peak locations to those found in solution scattering patterns (Figure S5). However, signal-to-noise was greatly increased and the acquisition time was decreased by using solid samples. X-rays of 11.11 keV were focused onto the sample, and a two-dimensional CCD array was used to collect the scattered X-rays after transmission through the sample. The signal was then radially integrated to obtain a 1D plot of intensity versus scattering angle.

Single Crystal X-ray Diffraction. Diffraction quality crystals were obtained by evaporation from a 3:1 mixture of ethanol and

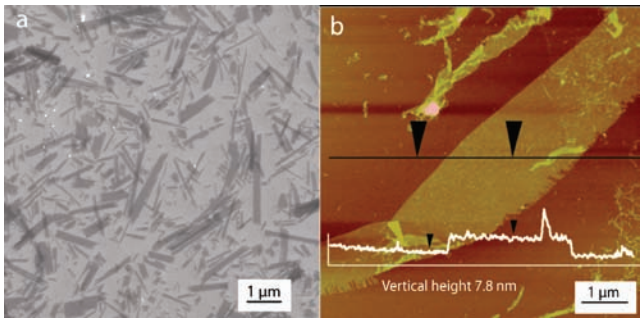

Figure 1. Sheet structures formed from the diblock copolypeptoid $p\text{Npe}_{15}\text{Nce}_{15}$ after 24 h in an aqueous solution at pH = 6.8. Scanning electron microscopy in backscatter electron mode (a) and atomic force microscopy (b) were used to observe these structures. AFM analysis determined the thickness of the sheets to be 7.8 ± 0.53 nm.

water at 0.7 mg/mL. Data were collected on 1,4-diphenethylpiperazine-2,5-dione crystal that was a colorless plate with dimensions $0.12 \times 0.10 \times 0.04$ mm^3. Data reduction was performed using SAINT and SADABS, and the structure was solved by SIR-2004 and refined with SHELXL-97.

Results and Discussion

Aromatic−aromatic interactions play a central role in the self-assembly of both biological and synthetic macromolecules. For example, in the case of polypeptides, it is known that a sequence as short as a dimer of phenylalanine can form remarkably robust nanotube structures.[42,43] Additionally, β-sheet fibrils can be readily formed from short peptide sequences containing a combination of ionic and aromatic residues.[16,44,45] Therefore, we designed our model polypeptoid diblock to include a single hydrophobic aromatic block containing 15 2-phenethyl side chains and a single hydrophilic ionic block containing 15 2-carboxyethyl side chains, resulting in *N*-(2-phenethyl)glycine-*b*-*N*-(2-carboxyethyl)glycine, $p\text{Npe}_{15}\text{Nce}_{15}$ (Table 2). In addition to containing the aromatic and ionic groups known to be important in polypeptide self-assembly, this molecule is also analogous to poly(styrene-*b*-acrylic acid), one of the most well studied chargeable amphiphilic synthetic block copolymers.

After automated synthesis and HPLC purification, $p\text{Npe}_{15}\text{Nce}_{15}$ was dissolved in water at a concentration of 0.1 mM and the pH was adjusted to 6.8 using 0.5 equiv of NaOH per carboxyl side chain. Sheet-like structures formed within 24 h and were imaged using scanning electron microscopy (SEM, Figure 1a) and atomic force microscopy (AFM, Figure 1b). The sheets range from several hundred nanometers up to many micrometers in length and width, and their edges appear quite straight. AFM analysis of 10 sheets showed the sheet thickness to be very uniform at 7.8 ± 0.53 nm. Given that the fully extended length of a single peptoid chain is approximately 11 nm, it is thought that the sheets consist of interdigitated bilayers. In this scenario, the hydrophobic portion of the molecule is embedded in the interior of the sheet in order to minimize contact with water while the charged hydrophilic block faces outward, exposed to the aqueous solution (Figure 2). Superhelical structures appear after 4−7 days in solution (Figure 3).

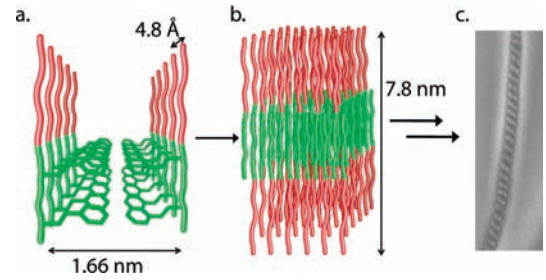

Figure 2. A model of the proposed self-assembly process. The green represents the hydrophobic portion of the chain while the red represents the hydrophilic block. The chains initially crystallize with the aromatic groups facing each other (a). This spacing (1.66 nm) along with the distance between two chains laterally (4.8 Å) are verified in X-ray scattering. The chains further arrange into two-dimensional sheets (b) with a height of 7.8 nm as verified by AFM and X-ray scattering. The sheets are layered within the helices as evidenced by lamellar X-ray scattering of the fully formed superhelices. The exact mechanism for the assembly of superhelices from the sheets is difficult to ascertain due to the lack of observed intermediate structures.

Over this transitional period, no intermediate structures between the sheets and helices were observed. However, the coexistence of sheets and helices in the same sample has been observed, indicating that any intermediate structure must be relatively short-lived. The wide time range of self-assembly indicates there are many competing pathways.

The superhelical structures are abundant and stable after formation, lasting many months in solution. Over 83% of the input peptoid mass is present in the final self-assembled helical structures (filtration and HPLC analysis, Supporting Information Figure S2). Analysis of 100 SEM images of the helices shows assemblies with surprisingly uniform helix diameters of 624 ± 69 nm and lengths ranging from 2 to 40 μm. These large dimensions are striking given the relatively small molecular weight (4371 g/mol) of the constituent building blocks. There are some examples of block copolymer assembly into large supramolecular helices with lengths of several micrometers,[46,47] but those helices are much smaller in diameter than the superhelices presented here. The superhelices presented here are most likely double helices based on analysis of the pitch angle and height (Figure S6). The helix half-pitch (606 ± 105 nm) is quite regular, and perhaps most remarkably, while the base polymer is achiral, the giant superhelices are homochiral, with all helices studied here having left-handed symmetry. A gallery of electron microscopy images of helices is presented in the Supporting Information (Figure S7).

Internal Structure. The regularity of the superhelix structure as seen in TEM, SEM, and AFM is indicative of internal ordering on the nanometer scale. Synchrotron X-ray scattering was used to probe this internal ordering. As shown through X-ray diffraction, repeat integer peaks starting at $q^* = 0.79$ nm^{-1} (labeled peak 1 on the solid curve in Figure 4) indicate an internal lamellar spacing within the helices with a *d*-spacing of 7.8 nm. This lamellar spacing closely matches the measured height of the sheets by AFM (Figure 1b). From this similarity it is hypothesized that these sheets are stacked within the helices, creating the lamellar peaks in X-ray scattering. However, due to the lack of observation of intermediate structures, it is difficult to understand how the sheets transition from single sheets into

(42) Reches, M.; Gazit, E. *Science* **2003**, *300*, 625–627.
(43) Smith, A. M.; Williams, R. J.; Tang, C.; Coppo, P.; Collins, R. F.; Turner, M. L.; Saiani, A.; Ulijn, R. V. *Adv. Mater.* **2008**, *20*, 37–41.
(44) Zhang, S. G.; Holmes, T.; Lockshin, C.; Rich, A. *Proc. Natl. Acad. Sci. U.S.A.* **1993**, *90*, 3334–3338.
(45) Pashuck, E. T.; Stupp, S. I. *J. Am. Chem. Soc.* **2010**, *132*, 8819–8821.
(46) Dupont, J.; Liu, G. J.; Niihara, K.; Kimoto, R.; Jinnai, H. *Angew. Chem., Int. Ed.* **2009**, *48*, 6144–6147.
(47) Zhong, S.; Cui, H. G.; Chen, Z. Y.; Wooley, K. L.; Pochan, D. J. *Soft Matter* **2008**, *4*, 90–93.

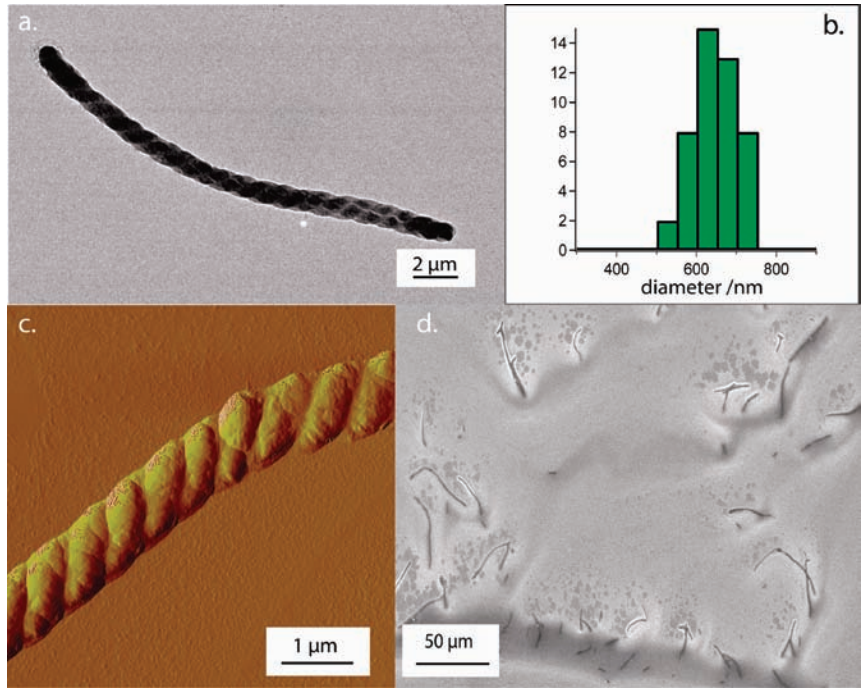

Figure 3. Helix formation from $p\text{Npe}_{15}\text{Nce}_{15}$ occurs after 3−7 days in aqueous solution at a pH of 6.8. The helices are 624 ± 69 nm in diameter (the histogram is shown in b) and range from 2 to 40 μm in length. They can be seen in TEM (a), AFM (c), or SEM in backscatter electron mode (d). A zoomed out image (c) shows the abundance of the structures within one sample.

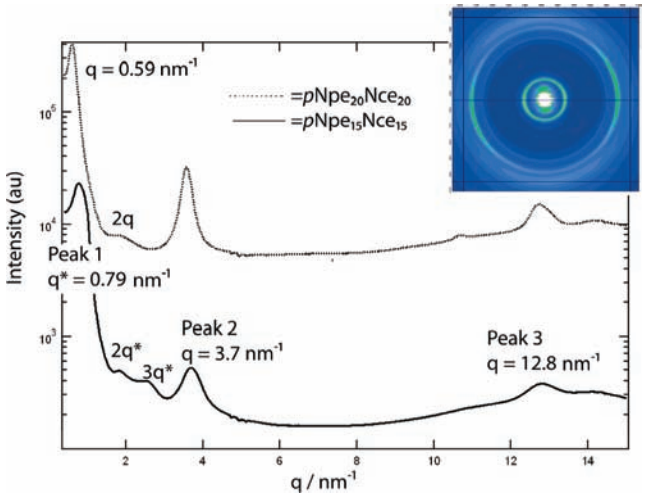

Figure 4. Synchrotron X-ray scattering was performed on an evaporated helix sample to investigate the internal ordering. The dotted line here represents $p\text{Npe}_{15}\text{Nce}_{15}$ while the solid line is $p\text{Npe}_{20}\text{Nce}_{20}$. The peaks marked q*, 2q*, and 3q* indicate a lamellar stacking with a *d* spacing of 7.8 nm, very similar to the thickness of the sheets. The peaks marked 2 and 3 are crystalline peaks at *d* spacings of 1.66 nm and 4.8 Å respectively and are hypothesized to be intrachain packing as modeled in Figure 1.

stacks within a double helix. In addition, there are also peaks at $q = 3.7$ and 12.8 nm^{-1} which correspond to *d*-spacings of 1.66 nm and 4.8 Å (labeled peaks 2 and 3 respectively in Figure 4). These peaks are attributed to crystalline packing between chains (Figure 2a). The 1.66 nm dimension corresponds to the distance between two chains packed inside the supramolecular helix (side chain crystallinity) with the 2-phenethyl groups facing each in other in what is most likely an edge-to-face orientation as seen in Figure 2a. The 4.8 Å dimension corresponds to the neighboring interbackbone distance as shown in Figure 2a.

An anisotropic 2D scattering pattern (Figure 4, inset) supports the model put forth in Figure 2. Importantly, the crystalline peaks are perpendicular to the lamellar peaks (the arc at the lowest *q*) as would be expected from the model in Figure 2. Due to the presence of multiple grains and the twisting of the helix, both of the crystalline peaks are seen in the meridional direction even though in any individual sheet they are perpendicular to each other. The anisotropy appears in the scattering only after centrifugal (as opposed to static) evaporation, indicating the centrifugation causes some partial alignment of the helices. The scattering pattern is similar to that observed in amyloid fibrils[48−50] and helices formed from amyloid β peptide fragments[51] where the meridional peaks are cited as evidence of a cross-β structure.

To further confirm the assignment of the lamellar and intramolecular crystalline peaks, specific chemical modifications were made to both the main chain and the side chain lengths of the polymer. The resulting changes in the X-ray scattering peaks were used to verify the origin of the peaks. First, the overall length of the polymer was increased from 15 monomers of each block to 20 monomers of each block forming the 40mer $p\text{Npe}_{20}\text{Nce}_{20}$. This had the effect of decreasing the *q*-value for the primary peak, q*, from 0.79 nm^{-1} to 0.59 nm^{-1}, demonstrating an increase in the lamellar spacing by 2.64 nm (Figure 4, dotted line). This was corroborated by AFM analysis showing the thickness of the sheets formed by $p\text{Npe}_{20}\text{Nce}_{20}$ to be 9.9 ± 0.66 nm. The scattering and AFM confirmed that the lamellar q*, 2q*, and 3q* peaks do stem from polymer chains extended in the lengthwise direction and also that these lamellar peaks are linked to the sheet thickness. As predicted by the model in Figure 2, the location of the crystalline peaks between side

(48) Blake, C.; Serpell, L. *Structure* **1996**, *4*, 989–998.
(49) Sunde, M.; Serpell, L. C.; Bartlam, M.; Fraser, P. E.; Pepys, M. B.; Blake, C. C. F. *J. Mol. Biol.* **1997**, *273*, 729–739.
(50) Serpell, L. C. *Biochim. Biophys. Acta: Mol. Basis Dis.* **2000**, *1502*, 16–30.
(51) Castelletto, V.; Hamley, I. W.; Hule, R. A.; Pochan, D. *Angew. Chem., Int. Ed.* **2009**, *48*, 2317–2320.

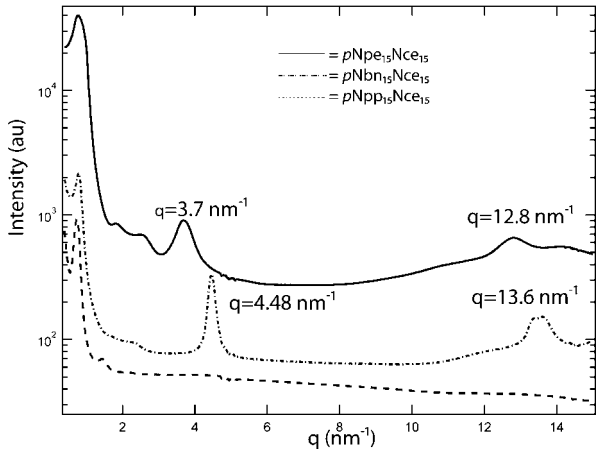

Figure 5. X-ray scattering on helical samples of $pNpe_{15}Nce_{15}$ (solid), $pNbn_{15}Nce_{15}$ (perforated), and $pNpp_{15}Nce_{15}$ (dashed). The lamellar peaks at $d = 7.8$ nm remain in each sample. However, in the $pNbn_{15}Nce_{15}$ sample, the crystalline peaks have shifted to higher q indicating a smaller spacing. The shift in the peak originally at 3.7 nm^{-1} has now shifted to 4.48 nm^{-1} which corresponds to two C−C bonds. The peak originally at 12.8 nm^{-1} has shifted to 13.6 nm^{-1}. It is not clear where the size of this shift originates.

chains (peaks 2 and 3 in Figure 4) was not altered by this chemical modification since they stem only from the packing of the side chains, which have not been changed in this case.

Additional chemical modifications were made to investigate the higher q peaks attributed to intrachain packing. The length of the 2-phenylethyl side chain was shortened by one methylene unit to create *N*-(benzyl)glycine-*b*-*N*-(2-carboxyethyl)glycine (pNbn$_{15}$Nce$_{15}$, Table 2). This molecule also forms a superhelix when self-assembled in aqueous solution. The peak which originally corresponded to a *d*-spacing of 1.66 nm shifts to reflect a *d*-spacing of 1.37 nm, resulting in a difference of 2.9 Å (Figure 5). This is reasonable given a C−C bond length of 1.54 Å and a crystalline arrangement with the phenyl groups facing each other such that a one carbon change in the side chain linkage actually results in a distance decrease of two carbon−carbon bonds (Figure 2). The peak originally corresponding to a 4.8 Å spacing shifts to a *d*-spacing of 4.5 Å. This peak, as shown in Figure 2a, does not depend directly on side chain length so it is likely that, with a smaller side chain, the backbones can simply pack slightly closer together. The length of the phenyl side chain was also increased by one methylene unit to form *N*-(3-phenylpropyl)glycine-*b*-*N*-(2-carboxyethyl)glycine (pNpp$_{15}$Nce$_{15}$, Table 2), which also formed superhelices. However, in this case the side chain crystalline peaks disappear, indicating that crystallization is not present within the helices (Figure 5). The longer side chains are more flexible and therefore more difficult to crystallize. This is corroborated by differential scanning calorimetry data (Supporting Information, Figure S5) indicating that the *N*-(3-phenylpropyl)glycine homopolymer does not crystallize in the solid state whereas the 2-phenethyl homopolymer does.[28] Crystallization of the hydrophobic block is therefore not an essential factor in the overall formation of the superhelices.

Simply using chemical modifications can only give indirect evidence of the atomic structure within the helix. To gain further insight into the details of the atomic order in the hydrophobic block, a model compound was synthesized and crystallized. Because symmetric cycloalkanes and *N*-methylated cyclic

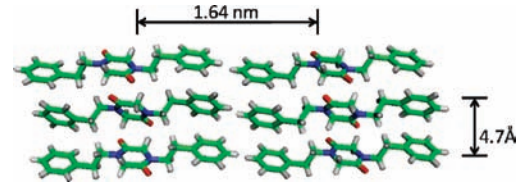

Figure 6. Crystal structure of a model cyclic dipeptoid 1,4-bis-(2-phenethyl)-piperazine-2,5-dione showing the packing geometry of the 2-phenylethyl groups. Green represents carbon atoms, blue represents nitrogen, red represents oxygen, and white represents hydrogen. The dimensions shown match those seen in X-ray scattering of a superhelix.

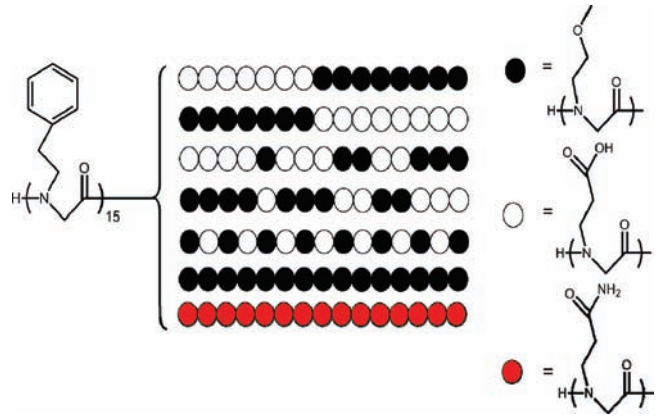

Figure 7. A set of closely related sequences was designed to pin the chargeable groups at specific locations. The hydrophobic portion of the molecule was held constant while the hydrophilic block was altered. The solid circles represent 2-methoxyethyl side chains which have a similar hydrophilicity to the carboxyethyl side chains (○) but cannot be charged. The red circles represent *N*-(2-carboxamidoethyl) side chains which have similar hydrogen bonding capabilities as the carboxyethyl side chains, but cannot be charged.

dipeptides have been shown to readily crystallize,[52,53] we prepared a cyclic dipeptoid, 1,4-bis-(2-phenethyl)-piperazine-2,5-dione, that displays the same *N*-2-phenethyl side chain groups present in the diblock. It is hypothesized that cyclized dipeptoids could serve as a model system to gain insight into the packing of these side chains within a larger structure. The atomic structure of the cyclic *N*-2-phenethyl dipeptoid was determined by X-ray crystallography (Figure 6) as a comparison to pNpe$_{15}$Nce$_{15}$.

The phenethyl groups are aligned with one another in a staggered edge-to-face conformation to form a plane (Figure 6). Lamellar stacks of these planes result in aromatic faces pointing directly toward each other. The spacings observed from the X-ray scattering of the pNpe$_{15}$Nce$_{15}$ helices (1.66 nm and 4.8 Å, respectively, Figure 4) match the dimensions shown in the diketopiperazine crystal structure corresponding to the side chain and main chain packing distances (1.64 nm and 4.7 Å, respectively, Figure 7a). Similarly, the spacings observed from the X-ray scattering of the pNbn$_{15}$Nce$_{15}$ helices (1.37 nm and 4.5 Å, respectively, Figure 5) match the side chain packing and the backbone (central ring) spacing dimensions shown in the

(52) Palacin, S.; Chin, D. N.; Simanek, E. E.; MacDonald, J. C.; Whitesides, G. M.; McBride, M. T.; Palmore, G. T. R. *J. Am. Chem. Soc.* **1997**, *119*, 11807–11816.
(53) Benedetti, E.; Marsh, R. E.; Goodman, M. *J. Am. Chem. Soc.* **1976**, *98*, 6676–6684.

previously reported[54] crystal structure of a 1,4-dibenzyl-piperazine-2,5-dione (1.34 nm and 4.5 Å, respectively). This is consistent with the shortening of the side chain by one methylene unit. The agreement of these structures with the X-ray scattering data for both the *N*-2-phenethyl and *N*-benzyl structures strongly supports the model proposed for the chain conformation within the lamellar stacks of the superhelix (Figure 2).

Ionic Interactions. The interplay of ionic interactions and hydrogen bonding of the carboxyethyl groups is clearly central to the self-assembly of the superhelices. These interactions can be exactly varied via side chain chemistry, solution interactions, and sequence control in the synthesis of the polypeptoids. Charge density and distribution were varied by adjustment of the solution pH as well as by side chain substitutions. Helix formation occurred in the buffered region from pH 5.5 to pH 9.5 of the molecule where between 1/2 and 2/3 of the carboxylates are charged (titration curve is shown in the Supporting Information, Figure S3). At high pH, only the sheet structures persist due to the high level of deprotonation of the carboxylic acids and the resulting electrostatic repulsion. At a pH less than 5.5, the molecule is not soluble and no organized self-assembly occurs. Therefore, some intermediate level of charge was necessary for superhelix self-assembly. Further study of the dependence of charge location on the formation of superhelices was performed by substituting a nonchargeable monomer of similar hydrophilicity, *N*-(2-methoxyethyl)glycine, at particular locations along the hydrophilic block, as shown in Figure 7. Given a fixed number of charges, the location of the charges does not affect helix formation. To investigate whether hydrogen bonding alone is sufficient to cause superhelix formation, a hydrogen bonding, but nonionic, side chain *N*-(2-carboxamidoethyl)glycine was used for the hydrophilic block ($p\mathrm{Npe}_{15}\mathrm{Nbm}_{15}$, Figure 7, red circles). Neither this sequence nor that made from an analogous nonionic non-hydrogen bonding side chain *N*-(2-methoxyethyl)glycine ($\mathrm{pNpe}_{15}\mathrm{Nme}_{15}$, Figure 7, black circles) self-assembles into organized structures, demonstrating that ionic interactions are indeed necessary for helix self-assembly to occur.

Chirality. Chirality is a ubiquitous presence in biomacromolecules resulting from the inherent chirality of the molecular building blocks (e.g. amino acids and nucleotides). Chiral helices in particular are observed throughout chemistry and biology due to their energetically favorable configuration of over simple columnar structures.[55] The existence and origins of biomolecular homochirality have been widely debated.[56−60] In addition, there are numerous examples of synthetic symmetry breaking systems in the literature[33,61−64] although the origin of the symmetry breaking in these systems is not always understood. In this study, the component polymers that make up the giant superhelices are completely achiral, making the resulting supramolecular homochirality an unusual and fascinating result. There are no chiral materials present in the self-assembly solutions, and yet, without exception all of the helices observed (hundreds) were left handed (see the Supporting Information for an image gallery, Figure S6). In previously reported examples of giant helices from block copolymers, the chirality has come from the molecular chirality of the polymer which is not present in this case. Additionally, chiral superstructures resulting from achiral building blocks are as a rule racemic mixtures or are influenced in a mechanical manner such as stirring. While we know of no other examples of homochiral superstructures resulting from achiral building blocks without external stimulation, supramolecular chirality can be affected by very subtle influences as evidenced by the significant body of research on the "sergeants and soldiers theory".[65] It has been shown that the introduction of a small number of chiral groups can cause an otherwise achiral entity to behave in a homochiral manner. One example of this is poly(alkyl isocyanate) molecules which self-assemble into chiral columnar stacks[65] when a small amount of chiral *N*-hexyl cyanate monomer is added. In a second example, a very small excess of a chiral side chain on one of the benzene groups in a *C*3 symmetrical benzene tricarboxamide can tip the self-assembly of these molecules such that a homochiral columnar stack results.[66−69]

With the sergeants and soldiers principle in mind, several analogs of the parent molecule were synthesized. Chiral groups were introduced at particular locations in the chain in an attempt to influence the supramolecular homochirality. It was thought that perhaps a trace chiral contaminant had been unknowingly introduced to the system and, by intentionally inserting a "sergeant", the chirality could be controlled and thus understood. Initially, a single chiral side chain was inserted at the interface of the two blocks. *N*-((*R*)-(+)-1-Phenylethyl)glycine (Nrpe) and *N*-((*S*)-(-)-1-phenylethyl)glycine (Nspe) were chosen for their similarity to Npe. The molecules created ($p\mathrm{Npe}_{14}\mathrm{Nrpe}_{1}\mathrm{Nce}_{15}$ and $p\mathrm{Npe}_{14}\mathrm{Nspe}_{1}\mathrm{Nce}_{15}$, Table 2) both formed left handed superhelices. With the hypothesis that perhaps one chiral group was not powerful enough to affect the overall structure, the entire Npe block was replaced with either Nspe ($p\mathrm{Nspe}_{15}\mathrm{Nce}_{15}$) or Nrpe ($p\mathrm{Nrpe}_{15}\mathrm{Nce}_{15}$) (see Table 1). Again, both of the resulting molecules formed identical left handed helix structures. In addition the molecule was synthesized in the reverse order, such that the N-terminal and C-terminal blocks were reversed ($p\mathrm{Nce}_{15}\mathrm{Npe}_{15}$, Table 2). The reasoning here was that perhaps the end groups were providing a source of asymmetry. However, left handed helix structures again assembled. Finally, rather than using an achiral counterion (NaOH) to adjust pH, (*R*)- or (*S*)-α-methyl benzyl amine was used, again resulting in left handed helices in both cases. The homochirality has proved remarkably robust as none of these approaches changed the overall superhelix chirality. It has been hypothesized that surface effects

(54) Nunez, L.; Brown, J. D.; Donnelly, A. M.; Whitlock, C. R.; Dobson, A. J. *Acta Crystallogr., Sect. E: Struct. Rep. Online* **2004**, *60*, O2076–O2078.
(55) Snir, Y.; Kamien, R. D. *Science* **2005**, *307*, 1067–1067.
(56) Breslow, R.; Levine, M.; Cheng, Z. L. *Orig. Life Evol. Biosph.* **2010**, *40*, 11–26.
(57) Mason, S. F. *Nature* **1984**, *311*, 19–23.
(58) Weissbuch, I.; Illos, R. A.; Bolbach, G.; Lahav, M. *Acc. Chem. Res.* **2009**, *42*, 1128–1140.
(59) Cintas, P. *Angew. Chem., Int. Ed.* **2008**, *47*, 2918–2920.
(60) Bonner, W. A. *Orig. Life Evol. Biosph.* **1991**, *21*, 59–111.
(61) Tsuda, K.; Alam, A.; Harada, T.; Yamaguchi, T.; Ishii, N.; Aida, T. *Angew. Chem., Int. Ed.* **2007**, *46*, 8198–8202.
(62) Link, D. R.; Natale, G.; Shao, R.; Maclennan, J. E.; Clark, N. A.; Korblova, E.; Walba, D. M. *Science* **1997**, *278*, 1924–1927.
(63) Wolffs, M.; George, S. J.; Tomovic, Z.; Meskers, S. C. J.; Schenning, A.; Meijer, E. W. *Angew. Chem., Int. Ed.* **2007**, *46*, 8203–8205.
(64) Mateos-Timoneda, M. A.; Crego-Calama, M.; Reinhoudt, D. N. *Chem. Soc. Rev.* **2004**, *33*, 363–372.
(65) Green, M. M.; Reidy, M. P.; Johnson, R. J.; Darling, G.; Oleary, D. J.; Willson, G. *J. Am. Chem. Soc.* **1989**, *111*, 6452–6454.
(66) Wilson, A. J.; van Gestel, J.; Sijbesma, R. P.; Meijer, E. W. *Chem. Commun.* **2006**, 4404–4406.
(67) Otani, T.; Araoka, F.; Ishikawa, K.; Takezoe, H. *J. Am. Chem. Soc.* **2009**, *131*, 12368–12372.
(68) Brunsveld, L.; Schenning, A.; Broeren, M. A. C.; Janssen, H. M.; Vekemans, J.; Meijer, E. W. *Chem. Lett.* **2000**, 292–293.
(69) Lightfoot, M. P.; Mair, F. S.; Pritchard, R. G.; Warren, J. E. *Chem. Commun.* **1999**, 1945–1946.

could account for the homochirality. However, self-assembly has occurred in both hydrophilic (glass) and hydrophobic (plastic) vials indicating that the surface probably does not play a large role in the self-assembly. As expected, circular dichroism of the superhelices has shown no optical rotation of light (Supporting Information, Figure S7) demonstrating that the chirality is not on a molecular length scale. The shape of the molecule is another potential source of asymmetry, and neutron scattering is being pursued as a future experiment to test this possibility. The last possibility is the presence of unequal surface stresses on the lamellae as they form. This has previously been shown to cause preferential bending of the lamellae in one direction or the other.[70−72] It is not clear in this case what would cause unequal surface stresses although they cannot be ruled out as a potential chirality inducer.

Conclusion

In conclusion, a remarkable homochiral biomimetic structure has been discovered resulting from the self-assembly of an amphiphilic partially charged diblock copolypeptoid of defined sequence. The hierarchical internal ordering of the assemblies has been characterized in detail using X-ray scattering coupled with precise chemical modifications. The crystal structure of a small model molecule supports the model of self-assembly. While the origin of the homochirality of these structures remains a mystery, it is clear that the interplay of hydrophobic and electrostatic forces is crucial to the formation of such a complex structure. The highly ordered microscale self-assembly described here demonstrates the power of polypeptoids to serve as an ideal system for engineering and understanding biomacromolecular self-assembly across several length scales.

Acknowledgment. This work was supported by the Office of Naval Research in the form of a Presidential Early Career Award in Science and Engineering (PECASE) for R.A.S. Polypeptoid synthesis and associated chemical characterization were performed at the Molecular Foundry, and XRD experiments were performed at the Advanced Light Source (ALS). Both are Lawrence Berkeley National Laboratory user facilities supported by the Office of Science, Office of Basic Energy Sciences, U.S. Department of Energy, under Contract No. DE-AC02-05CH11231. The authors thank Dr. James Holton and George Meigs for experimental assistance and Dr. Gary Ren for helpful discussions. H.K.M. acknowledges the Department of Defense for an NDSEG fellowship, and A.M.R. acknowledges the National Science Foundation for a graduate fellowship. J.N.J. acknowledges the Defense Threat Reduction Agency for financial support.

Supporting Information Available: Analytical HPLC and MALDI spectra for polypeptoids, quantification of self-assembly, base titration curve for *p*$Npe_{15}Nce_{15}$, comparison of X-ray scattering in the solid state and in solution, differential scanning calorimetry data, electron microscopy images, circular dichroism spectroscopy, and X-ray crystallography data for 1,4-bis-(2-phenethyl)-piperazine-2,5-dione. This material is available free of charge via the Internet at http://pubs.acs.org.

JA106340F

(70) Keith, H. D.; Padden, F. J. *Polymer* **1984**, *25*, 28–42.
(71) Lotz, B.; Cheng, S. Z. D. *Polymer* **2005**, *46*, 577–610.
(72) Ye, H.-M.; Wang, J.-S.; Tang, S.; Xu, J.; Feng, X.-Q.; Guo, B.-H.; Xie, X.-M.; Zhou, J.-J.; Li, L.; Wu, Q.; Chen, G.-Q. *Macromolecules* **2010**, *43*, 5762–5770.